mining

MDPI

Article

Transforming Copper Smelting Waste into Metal-Depleted Material via Density Separation and High-Temperature Settling

Aleksandar Mitrašinović [1,*] and Dawei Yu [2,3]

[1] Institute of Technical Sciences of the Serbian Academy of Sciences and Arts, 11000 Belgrade, Serbia
[2] School of Metallurgy and Environment, Central South University, Changsha 410083, China
[3] National & Regional Joint Engineering Research Center of Nonferrous Metal Resource Recycling, Changsha 410083, China
* Correspondence: aleksandar.mitrasinovic@itn.sanu.ac.rs

Abstract

This research examines transforming contaminated mining waste into mineralogically stable material using density separation and high-temperature settling. Samples with elevated metal concentrations were collected from century-old landfill sites, separated from overburden and organic material, and subjected to density separation and thermal treatment at 1300 and 1400 °C. This process significantly reduced heavy metal content, lowering cumulative lead, cadmium, and arsenic concentrations from 2440 g/t to below 60 g/t, and efficiently removed volatile elements such as arsenic and zinc. Sulfur content decreased from 1.67 wt% to 0.21 wt% after treatment at 1400 °C, while oxygen content increased from 31.9 wt% to 36.29 wt% and 34.2 wt% after treatment at 1300 °C and 1400 °C, respectively. Mineralogical, differential thermal and chemical analyses confirmed the thermal stability of the resulting material up to at least 350 °C, with fayalite and magnetite as the predominant minerals. Final concentrations of heavy metals were below EU natural soil background levels, supporting the material's safe and sustainable reuse in environmental applications. By focusing on remediation of metal-rich hotspots, this approach enables practical reclamation of mining waste areas and supports the valorization of legacy copper slag deposits, advancing environmental restoration and circular economy goals.

Keywords: mining waste; density separation; settling; heavy metals; soil stabilization; environmental rehabilitation

Check for updates

Academic Editor: Claudio Oggeri

Received: 14 September 2026
Revised: 20 October 2026
Accepted: 21 October 2026
Published: 26 October 2026

Copyright: © 2026 by the authors. Licensee MDPI, Basel, Switzerland. This article is an open access article distributed under the terms and conditions of the Creative Commons Attribution (CC BY) license.

1. Introduction

Mining operations alter large areas of land, converting natural landscape into mining waste. These activities eradicate natural ecosystems and prevent agricultural activity by replacing nutrient-rich surface with inert or, more often, toxic tailings and overburden. To reverse this environmental degradation, minimizing the ecological footprint can be achieved through strategies that convert waste into functional foundation layer for industrial or urban development [1,2]. Converting mining waste into a usable material eliminates the need to extract natural surface material from other areas, supports land restoration for its intended purpose, and reduces dependence on expensive waste storage facilities and widespread landfilling [3,4].

Copper extraction generates substantial quantities of mine tailings, overburden, heap leach waste, smelter slag, and dust. When pyrite-type or other sulfide minerals, which are the primary copper-bearing minerals, are exposed to air and water, they can mobilize various metals and form sulfuric compounds that readily leach into the ground. Although

all mining waste alters the entire environment, the main are heavy metals contained in slags [5,6].

In areas affected by mining activities, heavy metals, elements characterized by an atomic density greater than 5 g/cm^3, constitute a major category of pollutants due to their pronounced toxicity, tendency to bioaccumulate, and the significant challenges associated with their removal from ecosystems. Some heavy metals, such as copper (Cu) and zinc (Zn), are essential in small quantities for the normal biological functions of plants and animals, but they become detrimental when their levels surpass specific thresholds, which vary depending on the metal and the affected organism. As a result, the term 'Potentially Toxic Elements' (PTEs) has become a prominent expression focusing on bioavailability and chemical structure, not just elemental density [7,8]. Toxic elements are nonessential chemical elements that cause adverse health effects even at trace levels. The most concerning heavy metals among all the PTEs are lead (Pb), cadmium (Cd), mercury (Hg), and metalloid arsenic (As), most of which are released primarily through anthropogenic activities, e.g., by mining into the ground, and by fossil fuel combustion into the air [9]. Once released, they persist in the environment, bioaccumulate in food chains, and pose significant risks to human health.

Modern methods for processing copper slags focus on maximizing resource recovery and minimizing environmental impact. Innovative approaches, including direct reduction [10], selective carbothermal reduction [11], or electrowinning [12], are gaining traction not only for extracting metals from primary sources but also for efficiently recovering metals from slags. These integrated processing strategies not only enhance the economic value of copper slags but also contribute to sustainable waste management. However, large amounts of legacy mining waste occupy considerable land areas, typically near human habitats.

This study investigates the feasibility of converting legacy copper-smelting waste into metal-depleted material via high-temperature settling. Selected samples with high heavy metal concentrations were collected from old landfill sites, separated from overburden and organics, and then underwent density separation. The mineral-rich fraction was thermally treated at 1300 and 1400 °C. After separating the overburden and organic materials, XRD and chemical analyses were performed on the mineral-rich portion where the heavy metals are contained.

2. Location, Methods, and Materials

Samples were collected from the plain land situated near the downtown area and to the south-west of the smelting operations. This site, once a natural ravine, convenient for flotation and smelting operations, served as a tailing pit and dumping site (Figure 1). Its proximity to residential neighborhoods and its impact on local ecosystems have made it a focal point of investigations (Figure 2a), resulting in a large property database of for both original base land and current waste field land, including Life Cycle Assessment (LCA) [13] and Techno-Economic Assessment (TEA) [14,15].

Significant variation exists in the type of mining waste and, consequently, in the chemical composition of the affected landscape. In the Bor municipality, 207 Mt of flotation tailings, 450 Mt of overburden, and 23 Mt of slag have accumulated and are often disposed of together at the same sites [16]. A cluster sampling strategy was employed to obtain representative samples from areas with the highest heavy-metal concentrations. The study area (Figure 1) was divided into several clusters based on surface characteristics and evidence of metallic mineralization. Sampling points within each cluster were chosen according to the degree of mineralization to ensure inclusion of zones with elevated contamination. Fifty batches were collected by piling material from depths between 0.5 and two meters (Figure 2c), yielding approximately 100 kg in total. After collection, all subsamples from

each batch were combined on a clean plastic sheet using coning and quartering, with repeated flattening and recombination, to achieve a uniform and representative mixture. The homogenized samples were subsequently transported to the laboratory, where they were crushed and ground in alumina mortars to particle sizes below 2000 µm with a median particle size at 670 µm (Figure 2d), thereby facilitating effective liberation of individual mineral phases and optimizing the subsequent settling process.

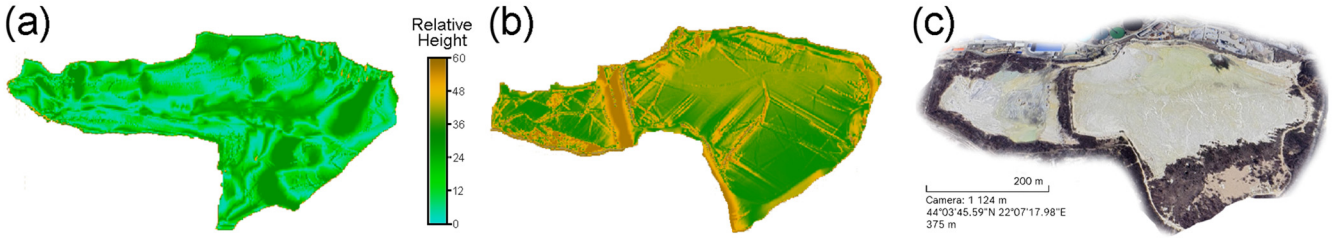


Figure 1. Transformation of the landscape. (**a**) Base resembling the original surface showing the starting ground level before any mining waste was added, (**b**) the top surface after mining waste material was placed on top of the base, and (**c**) Google Earth image used for modeling at a 60° tilt angle and 46° heading direction.

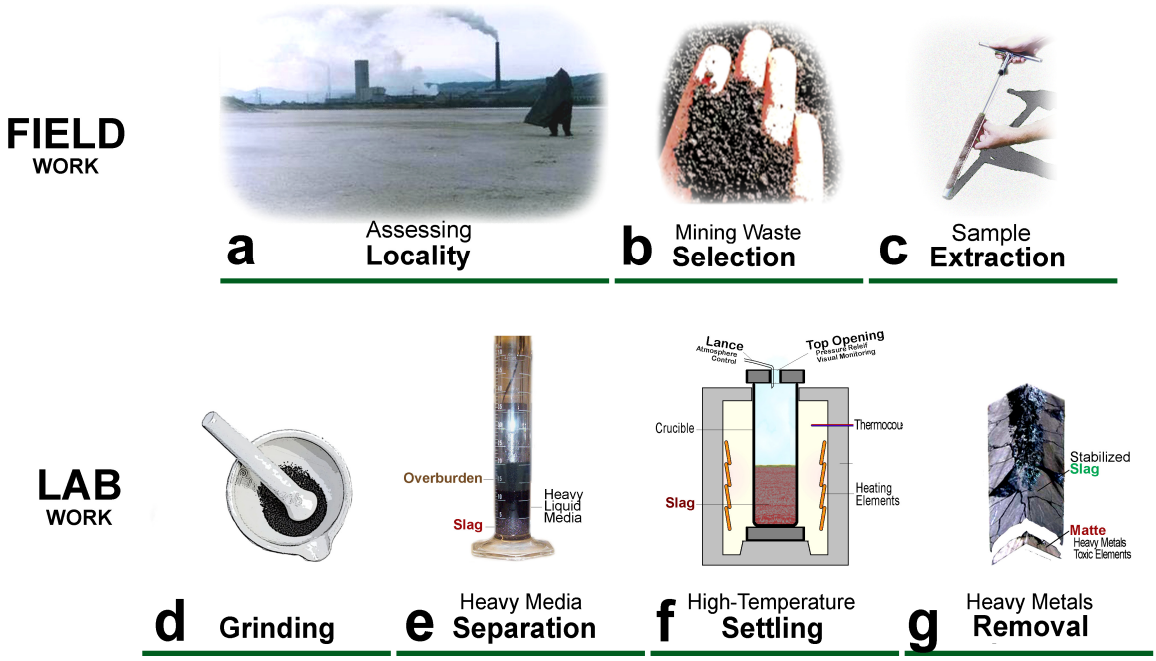


Figure 2. Procedure for removing heavy metals from mining waste generated during copper extraction.

Heavy liquid media (HLM) separation is a widely used mining separation technique in which heavier valuable ore particles sink while lighter waste material floats [17]. Lithium metatungstate ($Li_6(H_2W_{12}O_{40})$) (LMT) is a non-toxic, non-flammable, and more adjustable alternative to traditional organic heavy liquids [18], easy to recover by washing the suspension at temperatures below 90 °C, and recently used for the recovery of precious [19] and strategic [20] metals. Following crushing, the material underwent density-based separation using a solution of LMT. The separator was set to a density of 2.85 g/cm^3, a viscosity of 10 cP, and a solid-to-liquid ratio of 1 to 10, optimizing conditions for partitioning minerals from organic and other non-mineral fractions (Figure 2e). The one-step separation stage enabled removal of overburden and spoil, leaving mineral-rich particles that retained the majority of the potentially harmful metals present in the dump field. From the mineral-rich portion

collected at the bottom of the HLM separator, a small aliquot was taken for mineralogical and chemical analyses, while the remaining portion was conveyed for settling.

The typical chemical composition of copper slag closely aligns with the congruent point of fayalite, characterized by an FeO-SiO_2 ratio of 2:1, corresponding to 54.81 wt% Fe, 13.78 wt% Si, and 31.41 wt% oxygen. While elevated temperatures enhance metal coalescence, adjusting the chemical composition and temperature near the congruent point (1205 °C) enables operation at minimum process costs. In industrial applications, the optimal balance between metal coalescence and energy cost is achieved at around 1300 °C.

Maintaining a settling temperature of 1300 °C for the material with a fayalite-dominant mineralogy represents the ideal economic and operational spot in pyrometallurgical copper extraction. Assuming a power cost of 0.15 U$/kWh, a process efficiency of 10%, and a heat loss of 1440 kWh/h, the estimated total cost to increase and maintain a temperature of 1300 °C per hour is $44.50 per tonne [21]. This specific temperature balances fluid dynamics, phase stability, and energy consumption to minimize overall processing costs. The primary economic goal of a settling furnace is to let tiny, suspended droplets of dense copper matte or metallic copper separate physically from the lighter silicate slag phase [22]. According to Stokes' Law, the settling velocity of these droplets is inversely proportional to the slag's dynamic viscosity [23]. Below 1300 °C, viscosity increases sharply due to initial micro-crystallization. Raising the temperature to 1300 °C keeps the slag fully liquid with an exceptionally low viscosity [24]. This low resistance allows metallic droplets to coalesce and settle rapidly. Accelerating settling velocity reduces the required retention time in the settling or electric furnace. Shorter retention times translate directly to higher plant throughput and lower capital expenditure on oversized holding vessels. Increasing the temperature above 1300 °C improves fluid dynamics and reduces mechanical entrapment of metallic droplets, but it also shifts thermodynamic equilibria toward higher chemical solubility, meaning fewer metals will coalesce in the matte [25]. Molten fayalite is also highly aggressive, and as the temperature rises, the rate of chemical dissolution of the refractory material increases exponentially. Accordingly, in this study, the selected operating temperatures were 1300 °C and 1400 °C.

Particles from the bottom of the HLM separator were placed into a cylindrical alumina crucible measuring 17 cm in height and 3.8 cm in inner diameter (Figure 2f). To prevent uncontrolled oxidation by atmospheric oxygen, the crucible was flushed with argon gas throughout the experiment. Once loaded, it was heated to set temperature (1300 °C and 1400 °C) at a heating rate of 5 °C per minute. This heating process minimized thermal shock on the refractory material, enabling complete melting and promoting the separation of metallic phases. The high-temperature treatment lasted 4 h, allowing sufficient time for chemical reactions, phase separation, and settling of heavier material [26]. After this period, the crucible was removed from the furnace and left to cool naturally in ambient conditions until it reached room temperature. Upon cooling, the solidified samples were detached from the crucible. As shown in Figure 2g, the interface between the matte (metal-rich phase) at the bottom and the slag (oxidic phase) above is clearly defined, enabling the physical separation of these two products.

The mineralogical analyses of the initial material collected from the site and stabilized slag were determined using a PW 1830/40 X-ray Diffractometer (Philips, Almelo, The Netherlands) operating at 40 kV and 20 mA. The XRD scans were performed over a 2θ range of 10 to 90 degrees with a step size of 0.1 degrees, allowing the identification of crystalline phases present before and after treatment.

An electron probe micro-analyzer (EPMA) system comprising a Hitachi S-570 scanning electron microscope equipped with a Cameca SX50 microprobe was used to quantitatively detect the concentrations of metallic elements. The spatial resolution below 5 μm allows

measurement sensitivity ranging from 5 to 100 ppm_{wt} for elements from boron to uranium. Prior to analysis, samples were mounted in epoxy resin, polished, and coated with a thin conductive layer to prevent charging effects under the electron beam. Elemental mapping across wide areas and point analyses were performed to reveal partitioning, associations, and concentrations of metals within both the matte and newly formed slag. A multi-pass protocol was established to enable high-precision trace element analysis of the fayalite structure. The initial pass used a 20 kV accelerating voltage and a 30 nA probe current to detect major elements. Subsequent passes used a 25 kV accelerating voltage and probe currents of 50–500 nA to detect trace elements.

The thermal stability of various mineral phases, along with the impact of high-temperature treatment on phase composition, was evaluated using a Setaram TG92-16 Thermogravimetric Analyzer. Both differential thermal analysis (DTA) and thermogravimetric analysis (TGA) were conducted simultaneously at controlled heating rates of 10 and 20 °C/min.

3. Results and Discussion

Understanding the chemical bonding and elemental partitioning of the mining waste is crucial for selecting metal recovery processes. A combination of mineralogical and chemical analyses provides insights into the behavior of both valuable and heavy metal components of the mining waste under various conditions.

3.1. Mineralogical Characteristics

Figure 3a shows the X-ray diffraction analysis of the collected samples after removing the overburden, indicating the presence of a complex mineralogical structure consisting of quartz, fayalite, magnetite, pyrite, and kaolinite. Most of the quartz and kaolinite originated from ore-concentrating processes before being subjected to pyrometallurgical treatment, while fayalite and magnetite are byproducts of the converting operations [27]. Figure 3b shows the diffraction pattern of the newly formed slag after heating to 1400 °C, indicating that fayalite and magnetite are the dominant phases, which is consistent with typical copper slags. Qualitative analyses show that quartz remains in the final structure, with its peaks in the treated slag reduced to about half their original intensity, while magnetite-related peaks increase. However, during the settling process, kaolinite and pyrite phases undergo thermal decomposition during settling, accompanied by the pronounced crystallization of fayalite.

The predominance of complex oxide mineral forms in slags results from high-temperature metallurgical processes that favor the formation of stable compounds. Iron and silicon readily combine with oxygen to form stable phases that encapsulate other elements [28]. Silicon, present mainly as silica (SiO_2), is inert in the solid state but, depending on its amount, due to its high melting point and basicity, significantly shapes the thermal behavior of the mineral-rich portion of mining waste.

3.2. Thermochemical Analyses

Figure 4 depicts the non-isothermal thermogravimetric analysis (TGA) and differential thermal analysis (DTA) of investigated material in an oxygen–nitrogen atmosphere with 21% oxygen content at heating rates of 10 and 20 °C/min.

The thermogravimetric results demonstrate that, regardless of the applied heating rate, the sample's weight remains constant up to temperatures near 350 °C. This stability suggests that no significant decomposition, oxidation, or volatilization occurs in this lower-temperature region and confirms that, at temperatures below 350 °C, no structural changes occur. After surpassing this threshold, a steady increase in sample weight is observed, with

the maximum weight attained at around 870 °C. The initial weight gain, which begins just above 350 °C, is attributable to the oxidation of magnetite (Fe_3O_4) into hematite (Fe_2O_3) [29].

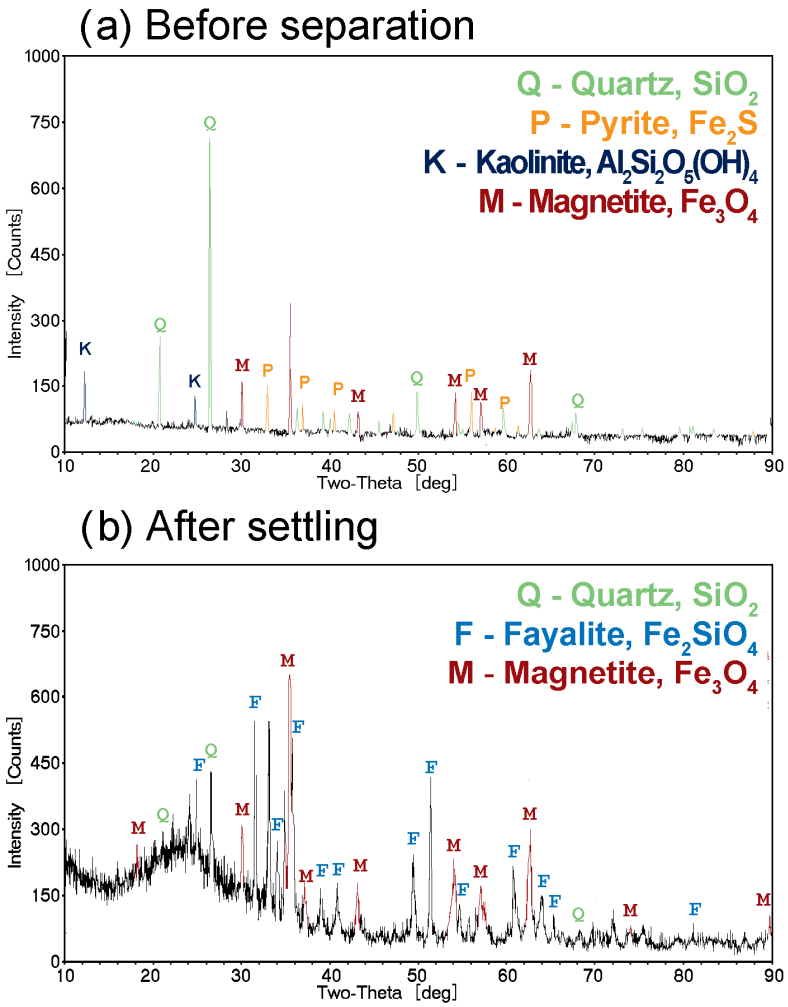


Figure 3. X-ray diffraction analysis of the overall treated material composition (**a**) and stabilized material after separation and settling (**b**).

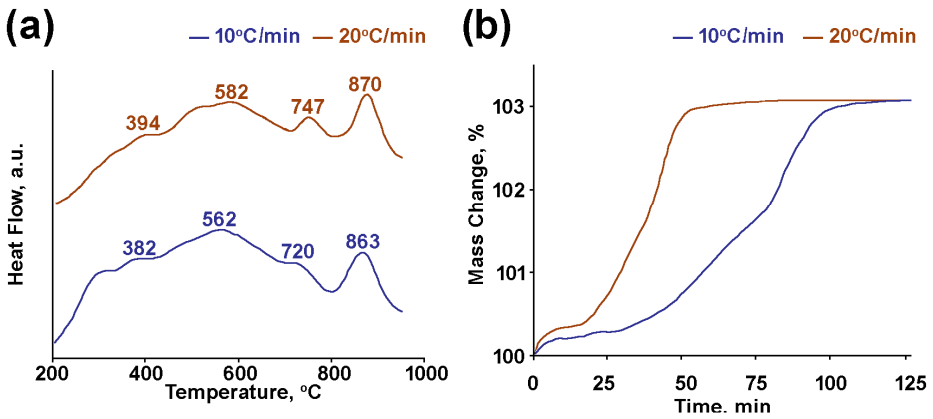


Figure 4. TGA/DTA curves of treated material immobilization by non-isothermal oxidation in atmospheric conditions. (**a**) DTA curves and (**b**) corresponding TGA curves.

Results of thermogravimetric analyses are further corroborated by differential thermal analysis data, which show a broad exothermic effect spanning from 350 to 1000 °C, indicating that multiple overlapping reactions and phase changes occur as the temperature increases.

The exothermic peaks observed in the DTA curves within the temperature intervals of 540–585 °C and 720–750 °C correspond to significant phase transformations: the first peak is associated with the conversion of magnetite to maghemite (γ-Fe_2O_3), and the second with the subsequent transformation of maghemite to hematite (α-Fe_2O_3). The appearance of exothermic peaks near 860 °C indicates the oxidation of minor copper and iron sulfide phases. The oxidation of these sulfides not only contributes to overall weight gain but also modifies the treated material's physical and chemical properties, specifically by forming stable oxides.

The combined TGA and DTA analyses provide insights into the material's potential thermal behavior. The sequential oxidation and phase transformation processes that occur as the temperature increases reveal the complex interaction among mineral phases, but regardless of complexity, all changes lead to more stable compounds [30].

An important outcome from the TGA/DTA analyses is that treated material can be stabilized at temperatures below 1000 °C. This process relies exclusively on solid-state reactions, which significantly reduces energy consumption and fully preserves the refractory material. Although this method may be less effective at removing heavy metals compared to liquid-state treatment, it facilitates the decomposition of less stable components, the formation of oxide compounds, and ultimately improves the stabilization of the treated material.

3.3. Mass Balance: Matte vs. New Slag

After settling, the heavier elements formed a matte at the bottom of the crucible, with a new slag forming above it. The total matte recovered (Γ_{Matte}) can be determined using a mass balance equation:

$$\Gamma_{Matte} = (m_{Matte}/m_{Initial}) \times 100, \text{ wt\%} \quad (1)$$

where m_{Matte} represents the weight of the recovered matte, and $m_{Initial}$ denotes the weight of the initial charge, which weighed 400 g of the laboratory-scale sample. After settling at 1300 °C, the matte formed weighed 17.8 g, whereas at 1400 °C, it weighed 19.7 g, giving matte recovery values of 4.45% and 4.92% at 1300 °C and 1400 °C, respectively. Increasing the settling temperature from 1300 °C to 1400 °C increased matte recovery and promoted the separation of heavy metals from the slag and their coalescence into matte at the bottom of the crucible, while leaving the remaining slag depleted of these heavy metals. Tables S1 and S2 in the Supplemental Materials show the chemical compositions and calculated mass balances for each element, along with a figure showing the partitioning percentages of each element between the initial and treated materials (Figure S1).

3.4. Chemical Composition Analyses

Slags are complex materials, containing many elements and intricate microstructures. They often include nearly every element from the periodic table, making chemical analysis difficult. Electron probe microanalysis (EPMA) offers accurate elemental analysis across a wide concentration range, and advances in energy-dispersive X-ray spectrometry (EDS) enable reliable detection of minor and trace elements [31]. In materials like mineral-rich components of mining waste, analyzing all elements at once can eliminate the need for compositional normalization, simplifying mathematical modeling [32]. While EPMA offers high precision, it is important to consider potential compositional variability present in mining waste samples.

In standard pyrometallurgical processing of copper ore concentrates, around 95% of the metals are typically recovered, with the remainder forming fayalite-based slag [33]. However, when fayalite slags are maintained in a liquid state for four hours followed by slow cooling, there is notable coalescence of the residual metals, approximately 5% of the

initially unextracted fraction, leading to the formation of a matte phase rich in elemental and sulfide-bound metals. In a previous study focusing on the recovery of valuable metals and the assessment of the marketable value of removed metals, the application of reducing agents introduced a new trade-off, enabling the further removal of 74.6 wt% of the residual metals [34]. The analysis of the partitioning and successive removal of valuable and/or heavy metals is significant for both economic recovery and environmental safety. Gathered at the bottom of the samples comprise 4.45 and 4.92 wt% of the matte recovered which contain copper, nickel, or precious metals that can be recovered through secondary processing.

Removing the bottom section of the solidified sample leaves newly formed slag depleted of heavy metals [35]. Table 1 shows a single trial of element concentrations in the upper part of the samples, consisting of newly formed slag after HLM separation and settling. Elements not detected are excluded from further analysis, though trace amounts may remain.

Table 1. EPMA analyses of the upper part of the sample before and after settling for four hours. Elements from $_{5}$B to $_{92}$U are analyzed (only those detected are shown in the table).

				Heavy Particles After HLM Separation	Remaining Slag After Settling	
Element	**Unit**	**Detection Limit**	**Sensitivity**		**1300 °C**	**1400 °C**
Fe	wt%	0.1	0.05	49.85	47.94	51.13
O	wt%	nd *	nd	31.90	36.29	34.21
Si	wt%	0.05	0.01	11.12	10.85	10.95
Al	wt%	0.01	0.01	2.77	2.57	3.05
S	wt%	0.01	0.01	1.67	0.9	0.21
Cu	wt%	0.01	0.01	0.97	0.38	0.02
Cr	wt%	0.01	0.01	0.71	0.42	0.12
Te	wt%	0.01	0.005	0.23	0.13	0.02
Se	wt%	0.01	0.01	0.17	0.12	0.07
Ca	wt%	0.1	0.05	0.15	0.15	0.14
Hg	g/t	5	1	790	202	14
Pb	g/t	10	5	700	205	15
Mg	g/t	200	100	600	500	400
Cd	g/t	5	5	570	375	30
As	g/t	10	10	380	nd	nd
Zn	g/t	10	10	370	260	nd
Ni	g/t	50	10	310	220	140
Mn	g/t	100	100	200	200	nd
Mo	g/t	5	5	200	125	50
Sb	g/t	10	10	200	160	100
Co	g/t	10	10	100	60	20
Sr	g/t	10	5	100	55	20
Ba	g/t	5	5	70	40	5
Ti	g/t	50	50	50	50	50

* 'nd' denotes a result below the detection limit.

Oxygen and sulfur, though not metals themselves, play critical roles in the chemical binding of both major and minor elements, affecting the solubility and mobility of metals within the slag [36]. The predominance of oxidic metals indicates that the bulk of the slag is relatively inert, but careful monitoring and processing are necessary to mitigate the potential release of heavy metals during slag disposal or utilization. Heavy metals, such as lead, mercury, cadmium, and arsenic, accounted for 2440 g/t, concentrations that can pose risks if not removed or stabilized.

After the treatment, elements with low sublimation or melting temperatures, such as arsenic and zinc, were removed below the detection limits. These elements readily volatilize at elevated temperatures, facilitating their effective removal from both the molten and

solidified phases. Consequently, their concentrations in the final slag product are negligible but careful management of off-gases is required to prevent atmospheric emissions.

The removal of each element analyzed after treatment at 1400 °C is shown in Figure 5. Heavier elements, due to their higher density, tend to partition into the matte phase during settling, while lighter elements may remain dispersed in the remaining slag above the matte or be partially lost through volatilization [37]. This density-driven segregation provides an effective means of recovering metals into the matte while leaving the stabilized slag products depleted from heavy metals.

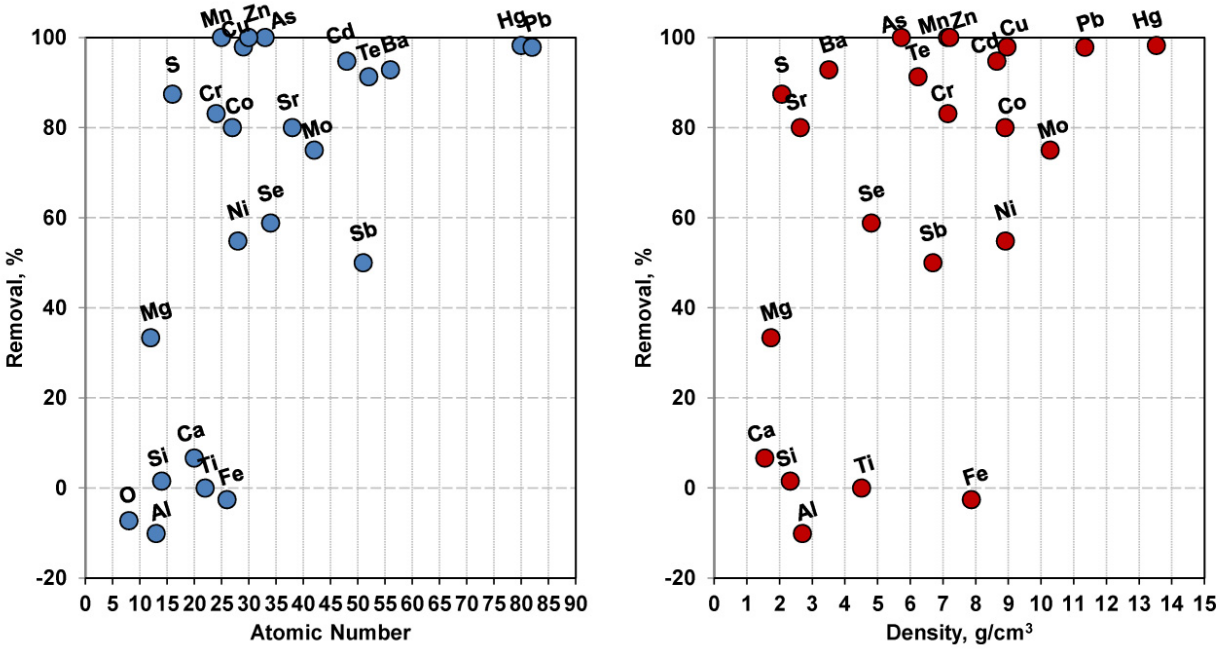


Figure 5. Removal of elements after high-temperature settling.

3.5. Elemental Patritioning Between Matte and Newly Formed Slag

During high-temperature treatment, most of the oxygen binds with elements such as iron and silicon to form stable oxide minerals, which are retained in the slag. This process stabilizes the slag and immobilizes unwanted elements by integrating them directly into the crystal lattices of stable, newly formed mineral phases. These host phases are highly resistant to environmental degradation, trapping elements inside their structures [38,39]. In contrast, sulfur reacts with residual metallic elements to form metal sulfide compounds, which are susceptible to leaching if disposed of [40].

The efficiency of metal extraction in pyrometallurgical processes is commonly evaluated by examining the partitioning of sulfur between slag and matte [41,42]. The sulfur capacity of the system is largely determined by the oxygen potential and temperature. Thermodynamically, as the matte grade increases, the partial pressure of sulfur decreases while that of oxygen increases, thereby reducing sulfur solubility in the slag [43]. This is favorable in terms of slag's cleanness, as sulfur tends to form a sulfide-rich matte, resulting in a low sulfur concentration in the oxide-rich slag phase. Although elemental sulfur is relatively non-harmful to humans, it can pose serious health risks when it reacts or combusts, producing volatile compounds such as sulfur dioxide (SO_2) or hydrogen sulfide (H_2S).

Alongside the significant reduction in heavy metal concentrations following the settling process, the sulfur concentration also decreased from 1.67 wt% to 0.21 wt%. This substantial reduction in sulfur is attributed to both physical separation during settling and chemical transformations, such as the oxidation of sulfide species or their incorporation into less

soluble mineral phases with densities higher those that of slag. Furthermore, analysis of the ternary diagram involving oxidic elements, sulfur, and heavy metals indicated a distinct displacement of heavy metals from the sulfur corner, as visualized in Figure 6. This shift suggests a preferential association of heavy metals with oxides rather than sulfur-containing phases. This process has important implications for the long-term stability of the treated material, which will eventually return to the environment, either as stabilized waste or as a value-added product.

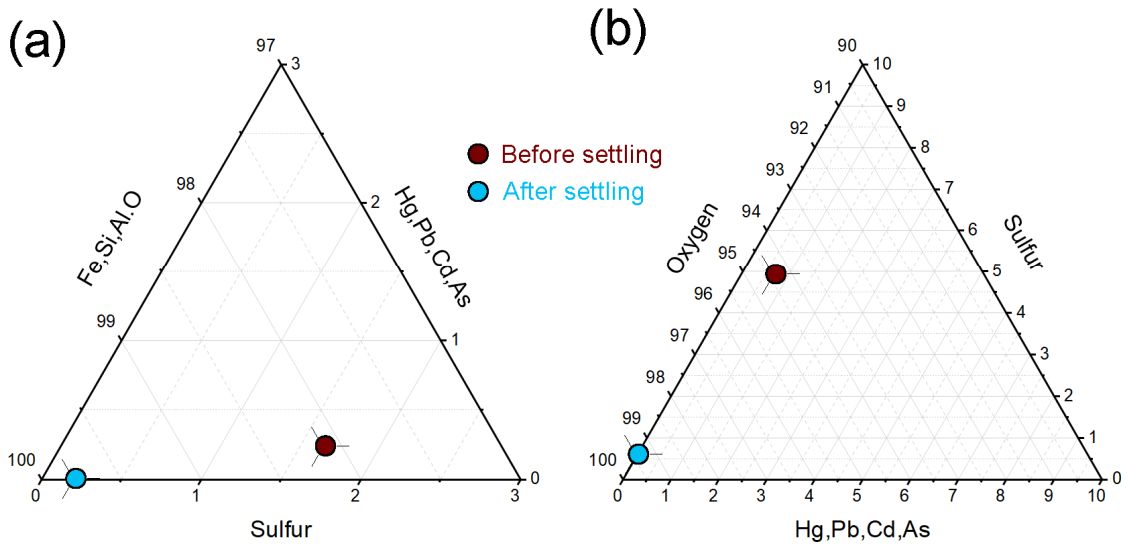


Figure 6. Elemental partitioning in the initial slag (**a**) and the newly formed slag (**b**) after settling at 1400 °C. Axis values are in %.

4. Process Applicability

The accumulated heavy metals in European soils exhibit substantial concentration differences, with pronounced regional variations driven by both natural and anthropogenic factors. Naturally, heavy metals concentrations are typically below 40 g/t in Scandinavian regions and exceed 100 g/t in mountainous areas of Greece. Figure 7 presents the concentrations of four heavy metals, arsenic (As), cadmium (Cd), mercury (Hg), and lead (Pb), demonstrating that the regional divergence in their concentrations from natural presence is primarily attributable to anthropogenic activities, such as mining and smelting, rather than to natural geological processes [44]. The region between Liege and Aachen in central Europe has the highest concentrations, likely the result of a long history of industrial activity, including mining, smelting, and manufacturing processes that have contributed to contamination over time [45]. In central UK, elevated levels of heavy metals are found in areas of high population density, where urbanization, transportation, and industrial emissions are known as significant contributors to pollution [46]. In Greece, elevated concentrations are associated with natural factors, such as frequent seismic activity and the exposure of lithosol, which enhance the mobilization and accumulation of heavy metals in the upper layers [47]. After settling, the combined concentration of four heavy metals in the analyzed samples (56 g/t) was well below the natural background levels typically observed in European soils.

The remaining slag, depleted of valuable and heavy metals, contained 20 to 30 wt% SiO_2, with the remainder primarily consisting of iron oxides. This composition aligns with the $2FeO{:}SiO_2$ phase, accounting for the predominance of fayalite as the major constituent in newly formed slag. Fayalite (Fe_2SiO_4) is a stable iron silicate that forms under the reducing conditions characteristic of copper pyrometallurgical processes. Its dominance as

the primary phase suggests that thermodynamic equilibrium was attained during the high-temperature treatment, resulting in the formation of a stable, inert structure. Although this laboratory study yields results for chemical processes aimed at reducing heavy metals, long-term field studies should be conducted to account for the seasonal variations in moisture and load-bearing capacity.

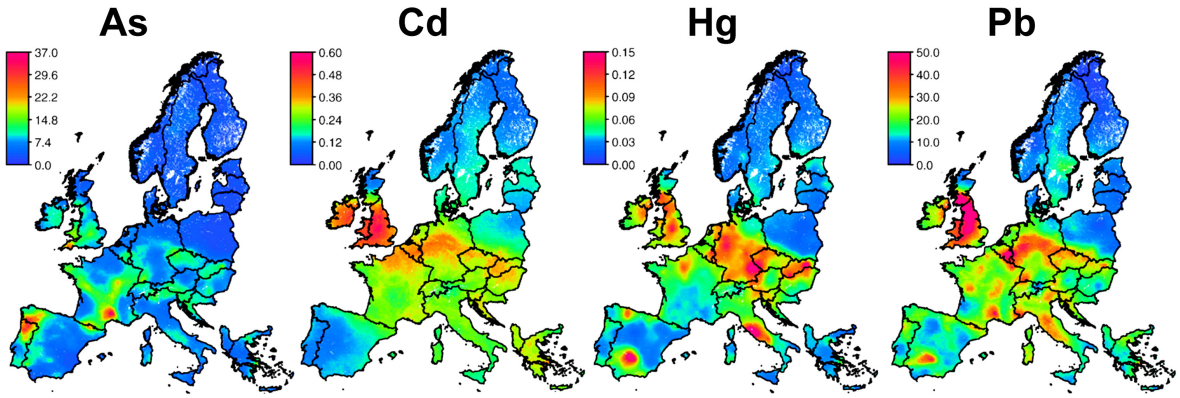


Figure 7. Concentrations of As, Cd, Hg, and Pb, mainly caused by anthropogenic factors. The image is in the public domain distributed by European Soil Data Centre (ESDAC): https://esdac.jrc.ec.europa.eu/themes/soil-contamination, (accessed on 20 October 2026).

Given the waste's origin, the most recent European Directive 2025/2360 should be applied, indicating that ISO 54321 standard [48] should be followed to assess the effects of residual heavy metals on the surrounding environment. The concentrations of all heavy metals accumulated in the matte at the bottom of the vessel and were subsequently collected for further valorization. Heavy metal concentrations in the remaining slag were significantly below the maximum levels permitted by EU regulations and the Regulation on Limit Values of Polluting, Harmful and Dangerous Substances in Soil of the Republic of Serbia [49]. The EU Soil Monitoring Law (Directive (EU) 2025/2360) does not set unified, legally binding limits for heavy metals in soil across the EU. Instead, it provides a framework for monitoring soil health with non-binding target values. Member States should set their own operational trigger values based on local conditions. In Serbia, these values are set as remediation values of 55, 12, 10, and 530 mg/kg for As, Cd, Hg, and Pb, respectively.

Conventional remediation strategies for mining waste, such as stabilization with cementitious binders, chemical immobilization, or phytoremediation, primarily aim to reduce contaminant mobility but often result in long-term storage of these unwanted substances. Hydrometallurgical and conventional pyrometallurgical metal recovery processes can achieve high extraction efficiencies but are energy-intensive, require chemicals, and generate secondary waste streams. In contrast, the combined density separation and settling process described here removes heavy metals and produces a mineralogically stable, metal-depleted material.

If differences are identified, engineered solutions such as blending disposed material with native soil or using liners and barriers may be implemented to harmonize the landfill material's behavior with the pre-existing geology [50,51]. These measures help maintain the integrity of the landscape, support safe construction or vegetation over reclaimed sites, and minimize risk to local flora, fauna, and water resources [52,53].

5. Conclusions

This study attempted to transform legacy mining waste into a mineralogically stable material through density separation and high-temperature treatment. Most heavy metals are

concentrated in the mineral-rich parts of mining waste, which, when brought to the liquid phase, separate further by density. Increasing treatment temperature significantly improves heavy metal removal efficiency. Higher temperatures accelerate chemical reactions and enhance heavy-metal removal, improving extraction or remediation. Key results include:

- The process removed heavy metals, resulting in a material without volatile species, with arsenic and zinc removed to below the detection limits.
- A significant reduction in heavy metal content. Mercury, lead, cadmium, and arsenic dropped from 2440 g/t to below 60 g/t.
- Sulfur content was reduced, and the final material showed increased oxygen content.
- Qualitative mineralogical analysis revealed a predominance of fayalite and magnetite, minerals with stable crystalline structures.
- The settling process preserved the refractory matrix of the treated material while promoting the decomposition of less stable components.

Removing heavy metals from contaminated sites offers a promising path for sustainable waste management in mining. These findings indicate the potential for converting mining waste into a material with modified mineralogical and chemical properties suitable for further applications.

Supplementary Materials: The following supporting information can be downloaded at: https://www.mdpi.com/article/10.3390/mining6040100/s1, Figure S1: Element partitioning between newly formed slag and matte after four hours of settling of mining waste; Table S1: Chemical composition and material balance of samples after separation of liquid media, newly formed slag, and matte at 1300 °C; Table S2: Chemical composition and material balance of samples after separation of liquid media, newly formed slag, and matte at 1400 °C.

Author Contributions: Conceptualization, A.M.; methodology, A.M.; validation, A.M. and D.Y.; formal analysis, A.M. and D.Y.; investigation, A.M.; writing—original draft preparation, A.M.; writing—review and editing, A.M. and D.Y.; visualization, A.M. All authors have read and agreed to the published version of the manuscript.

Funding: This research was funded by the Ministry of Science, Technological Development and Innovation, the Republic of Serbia, grant number 451-03-33/2026-03/200175.

Data Availability Statement: Data supporting the findings of this study are available from the corresponding authors upon reasonable request.

Acknowledgments: This research supports the United Nations Sustainable Development Goals as outlined in the document Transforming Our World: the 2030 Agenda for Sustainable Development, particularly SDG 7 (sustainable energy for all) and SDG 9 (inclusive and sustainable industrialization and innovation).

Conflicts of Interest: The authors declare no conflicts of interest.

References

1. Bommi, S.; Parameswari, E.; Dhevagi, P.; Janaki, P.; Davamani, V.; Sebastian, S.P.; Suganthy, M.; Krishnan, R.; Thirugnanasambandham, K. Transforming Mining Waste into Resources: A Review on Sustainable Construction and Agricultural Utilization. *Environ. Geochem. Health* **2026**, *48*, 54. [CrossRef] [PubMed]
2. Silva, B.M.; Queiroz, H.M.; Ferreira, A.D.; Ruiz, F.; Ferreira, T.O. Technosols Made from Iron Mine Tailings and Construction and Demolition Waste as an Alternative for Sustainable Solid Waste Management. *Land Degrad. Dev.* **2025**, *36*, 208–217. [CrossRef]
3. Zhang, D.; Huo, Y.; Ge, C.; Zhang, W.; Wang, S.; Jiang, C.; Zhang, X.; Ge, X. Sustainable Valorization of Solid Wastes into Functional Technosols: Enhancing Aggregate Stability. Bacterial Networks, and Plant Growth. *Sustainability* **2026**, *18*, 4098. [CrossRef]
4. Gryczak, M.; Gomes, T.; Angioletto, E.; Angioletto, E.; Petzhold, C.L.; Elyseu, F.; Raupp-Pereira, F.; Noni Júnior, A.; Zocche, J.J. Environmental Risk Assessment of Technosols Formulated with Calcined Pyrite-Rich Coal Gangue. *Energ. Ecol. Environ.* **2026**, *11*, 697–707. [CrossRef]

5. Xiang, C.; Zhu, F.; Jiang, J.; Zeng, J.; Gao, W.; Li, X.; Xue, S. Unraveling the Migration Behavior of Metal(Loid)s in a Smelting Site Contaminated by Deeply Buried Slag. *J. Hazard. Mater.* **2026**, *507*, 141777. [CrossRef] [PubMed]
6. Sabitova, A.; Mukiyanova, R.; Kassymova, Z.; Bayakhmetova, B. Development of a Secondary Use Method for Non-Ferrous Slags Metallurgy for Obtaining Mineral Fertilizers. *Int. J. Mol. Sci.* **2026**, *27*, 4470. [CrossRef] [PubMed]
7. Liu, K.; Qiu, H.; Li, X.; Fan, P.; Qi, S. Prediction of Potentially Toxic Trace Elements (PTEs) in Soil and Sediments Using Vis-NIR Spectroscopy: A Review. *Appl. Spectrosc. Rev.* **2026**, *61*, 117–145. [CrossRef]
8. Tziourrou, P.; Golia, E.E. Phytoremediation of Co-Contaminated Environments: A Review of Microplastic and Heavy Metal/Organic Pollutant Interactions and Plant-Based Removal Approaches. *Soil Syst.* **2025**, *9*, 137. [CrossRef]
9. Eissa, F.; Elhawat, N.; Alshaal, T. Comparative Study between the Top Six Heavy Metals Involved in the EU RASFF Notifications over the Last 23 Years. *Ecotoxicol. Environ. Saf.* **2023**, *265*, 11548. [CrossRef] [PubMed]
10. Kuang, B.; Tan, C.; Li, F.; Hu, J.; Dou, Z.; Yu, Y.; Gao, H.; Wang, H. A novel method for cleaning molten copper slag and efficiently recovering copper resources through reduction modification. *Process Saf. Environ. Prot.* **2026**, *2010*, 108649. [CrossRef]
11. Li, S.; Wu, Z.; Yang, L.; Zhou, X. Direct reduction of copper slag with H_2 and CO: Effects of $CaCO_3$ on reduction kinetics. *J. Taiwan Inst. Chem. Eng.* **2026**, *178*, 106371. [CrossRef]
12. Abdelgawwad, A.A.; El-Hadad, S.; Ibrahim, M.; Bhlol, M.; Dawood, O.M. Secondary Copper and Copper Alloys Refining Techniques: A Short Review. *Int. J. Mater. Technol. Innov.* **2026**, *6*, 86–98. [CrossRef]
13. Živković, Ž.; Panić, M.; Fedajev, A.; Veličković, M. The Challenges of Increasing the Copper Smelter Capacity on Ambient Air Quality in Bor (Serbia). *Water Air Soil Pollut.* **2023**, *234*, 82. [CrossRef]
14. Nikolić, I.P.; Milošević, I.M.; Milijić, N.N.; Mihajlović, I.N. Cleaner production and technical effectiveness: Multi-criteria analysis of copper smelting facilities. *J. Clean. Prod.* **2019**, *215*, 423–432. [CrossRef]
15. Ulniković, V.P.; Kurilić, S.M.; Staletović, N. Air Quality Benefits From Implementing Best Available Techniques in Copper Mining and Smelting Complex Bor (Serbia). *Water Air Soil Pollut.* **2020**, *231*, 160. [CrossRef]
16. Antonijević, M.M.; Dimitrijević, M.D.; Stevanović, Z.O.; Serbula, S.M.; Bogdanovic, G.D. Investigation of the possibility of copper recovery from the flotation tailings by acid leaching. *J. Hazard. Mater.* **2008**, *158*, 23–34. [CrossRef] [PubMed]
17. Mitrašinović, A.M.; Utigard, T.A. Copper Removal from Hypereutectic Cu-Si Alloys by Heavy Liquid Media Separation. *Metall. Mater. Trans. B* **2012**, *43*, 379–387. [CrossRef]
18. Galvin, K.P. Options for washability analysis of coal—A literature review. *Coal Prep.* **2006**, *26*, 209–234. [CrossRef]
19. Ormuž, J.K.; Žmak, I.; Ćurković, L. Selective Gold Recovery from Waste Electronics: A Speciation-Based Recycling Approach. *Materials* **2026**, *19*, 538. [CrossRef] [PubMed]
20. Essel Arthur, S.; Atta Mends, E.; Gargiulo, M.; Smith, Y.R.; Chu, P. Dense Media Separation for Mineral Carbonation and Enhanced Rare Earth Mineral Recovery. *ACS Sustain. Resour. Manag.* **2026**, *3*, 473–483. [CrossRef]
21. Mitrašinović, A.; Nešković, J.; Stjepanović, P.; Išek, J.; Praštalo, Ž.; Polavder, S. Cost-Effective Remediation of Slag Formed from Polymetallic Ores Rich in Nickel, Copper, and Cobalt by Reduction Settling Technique Using Readily Available Iron-Based Additives. *Sci* **2026**, *8*, 260. [CrossRef]
22. Isaksson, J.; Vikström, T.; Lennartsson, A.; Samuelsson, C. Influence of Process Parameters on Copper Content in Reduced Iron Silicate Slag in a Settling Furnace. *Metals* **2021**, *11*, 992. [CrossRef]
23. Huang, M.X. Hydrodynamic simulation of metal droplet settlement in molten slag. *Trans. Nonferrous Met. Soc. China* **2023**, *33*, 1244–1257. [CrossRef]
24. Ströbele, F.; Wenzel, T.; Kronz, A.; Hildebrandt, L.H.; Markl, G. Mineralogical and geochemical characterization of high-medieval lead–silver smelting slags from Wiesloch near Heidelberg (Germany)—An approach to process reconstruction. *Archaeol. Anthropol. Sci.* **2010**, *2*, 191–215. [CrossRef]
25. Jiayun, Z. Physical Chemistry of Metallurgical Process. In *The ECPH Encyclopedia of Mining and Metallurgy*; Kuangdi, X., Ed.; Springer: Singapore, 2024. [CrossRef]
26. Mitrašinović, A.M.; Wolf, A. Effect of Reductants on Valuable Metals Separation and Recovery from Copper Cliff Converter Slag. *High Temp. Mater. Process.* **2014**, *33*, 123–129. [CrossRef]
27. Weiss, J.; Munchen, D.; Lucas, H.B.F. Fayalitic Minerals and Slags (Part I): A Survey on Composition and Potential for Phases Design. *J. Sustain. Metall.* **2026**, *12*, 2365–2384. [CrossRef]
28. Alam, S.; Tolibov, B.; Akhmedov, M.; Khujamov, U.; Yarlakabov, S. Enhanced Extraction of Valuable Metals from Copper Slags by Disrupting Fayalite and Spinel Structures Using Sodium Sulfate. *Minerals* **2025**, *15*, 771. [CrossRef]
29. Rabadjieva, D.; Marinkov, N.; Kostova, Y.; Kovacheva, D.; Gyurov, S.; Tzvetkova, C.; Gentscheva, G.; Penkov, I. Effect of Oxygen Content on the Non-isothermal Oxidation of Waste Slag from Copper Production. *J. Int. Sci. Publ.* **2017**, *11*, 178–187.
30. Bipra Gorai, R.K.J.; Premchand. Characteristics and Utilisation of Copper Slag—A Review, Resources. *Conserv. Recycl.* **2003**, *39*, 299–313. [CrossRef]
31. Batanova, V.G.; Sobolev, A.V.; Magnin, V. Trace element analysis by EPMA in geosciences: Detection limit, precision and accuracy. *IOP Conf. Ser. Mater. Sci. Eng.* **2018**, *304*, 012001. [CrossRef]

32. Sun, B.; Dai, J.; Huang, K.; Yang, C.; Gui, W. Smart manufacturing of nonferrous metallurgical processes: Review and perspectives. *Int. J. Miner. Metall. Mater.* **2022**, *29*, 611–625. [CrossRef]
33. Shishin, D.; Tripathi, N.; Sineva, S.; Jak, E. Thermodynamic Modeling and Research for Processing Complex Concentrate Blends in Custom Copper Smelters for Maximum Revenue. *Processes* **2024**, *12*, 2820. [CrossRef]
34. Mitrašinović, A.M.; Yuankun, Y.; Stopic, S.; Radosavljević, M. Feasibility of Recovering Valuable and Toxic Metals from Copper Slag Using Iron-Containing Additives. *Metals* **2023**, *13*, 1467. [CrossRef]
35. Mitrašinović, A.M.; Stopic, S.; Yu, D. Removal of the heavy metals from copper slag by using carbonless additives. *Waste Manag.* **2024**, *187*, 218–224. [CrossRef] [PubMed]
36. Chenguang, B. Basicity and Acidity of Slag. In *The ECPH Encyclopedia of Mining and Metallurgy*; Kuangdi, X., Ed.; Springer: Singapore, 2024. [CrossRef]
37. Wan, X.; Zhou, L.; Chen, Z.; Shen, L.; Chen, M. Review on Pyrometallurgical Smelting Options for Recycling Precious and Platinum Group Metals from Secondary Resources. *Metall. Mater. Trans. B* **2025**, *56*, 6118–6144. [CrossRef]
38. Guo, Y.; Du, Y.; Wei, Y.; Zhao, D.; Zhang, H.; Deng, L.; Chen, H.; Zhao, M. Crystallization, microstructural evolution, heavy metals migration, and solidification mechanism of blast furnace slag glass-ceramics. *Ceram. Int.* **2024**, *50*, 18462–18472. [CrossRef]
39. Zhao, Z.; Wang, Z.; Peng, N.; Peng, B.; Liang, Y.; Qu, S.; Dong, Z.; Zeng, W. Copper Behavior and Fayalite Microstructure Changes Influenced by Cu_2O Dissolution. *Jom* **2019**, *71*, 2891–2898. [CrossRef]
40. Msumange, D.A.; Jampaiah, D.; Tardio, J.; Nilsson, M.; Arandiyan, H.; Bhargava, S.K. A Review of Nickel and Cobalt from Laterite Ores: Toward Sustainable Extraction Pathways for the Battery Industry. *J. Sustain. Metall.* **2026**, *12*, 1038–1069. [CrossRef]
41. Liu, W.; Liu, S.; Ling, H.; Li, C.; Jiao, F. Production of Nickel Matte from Saprolitic Laterite Ore by Sulfide Smelting with Pyrite. *Miner. Eng.* **2025**, *233*, 109658. [CrossRef]
42. Lu, B.; Zhang, T.; Guo, W.; Wu, P.; Ma, Y.; Ma, X.; Shen, Y. Recovery of Nickel, Cobalt and Copper from Nickel Slag by a New Process of Reduction-Sulfurizing Smelting. *Metall. Res. Technol.* **2026**, *123*, 114. [CrossRef]
43. Tian, M.; Klemettinen, L.; Chen, M.; Taskinen, P.; Tiljander, M.; O'Brien, H.; Lindberg, D. Correction to: Phase Equilibria and Trace Element Deportments in Fe–O–Al_2O_3–SiO_2 Slags and Molten Copper Matte at 1473 K (1200 °C), Fixed $p(O_2)$ and $p(SO_2)$, and Silica/Magnetite Saturation. *Metall. Mater. Trans. B* **2025**, *56*, 2164–2166. [CrossRef]
44. Lado, L.R.; Hengl, T.; Reuter, H.I. Heavy metals in European soils: A geostatistical analysis of the FOREGS Geochemical database. *Geoderma* **2008**, *148*, 189–199. [CrossRef]
45. Schulte, P.; Weber, A.; Keßels, J.; Lehmkuhl, F.; Schüttrumpf, H.; Esser, V.; Wolf, S. Morphodynamics and Heavy Metal Accumulation in an Artificially Built Near-Natural River (Inde, Germany). *J. Sediment. Environ.* **2024**, *9*, 117–133. [CrossRef]
46. Trujillo-González, J.M.; Torres-Mora, M.A.; Keesstra, S.; Brevik, E.C.; Jiménez-Ballesta, R. Heavy Metal Accumulation Related to Population Density in Road Dust Samples Taken from Urban Sites under Different Land Uses. *Sci. Total Environ.* **2016**, *553*, 636–642. [CrossRef] [PubMed]
47. Ustaoğlu, F.; Yazman, M.M.; Batan, N.; Yüksel, B. Disaster-Induced Toxic Metal Mobilization in Post-Earthquake Street Dust of Adıyaman, Türkiye: Pollution Indices, Receptor Model Source Apportionment, and Probabilistic Health Risk Evaluation. *J. Hazard. Mater.* **2026**, *506*, 141606. [CrossRef] [PubMed]
48. *ISO 54321:2020*; Soil, Treated Biowaste, Sludge and Waste. International Organization for Standardization (ISO) Central Secretariat: Geneva, Switcherland, 2020.
49. Regulation on Limit Values of Polluting, Harmful and Dangerous Substances in Soil. The Official Gazette of the Republic of Serbia, No. 30/2018 and EU Directive No. 86/278/EEC-1986. Available online: https://faolex.fao.org/docs/pdf/srb195301.pdf (accessed on 8 October 2026).
50. Upadhyay, R.K. Mining, Mineral Beneficiation, and Environment. In *Geology and Mineral Resources*; Springer Nature: Singapore, 2025; pp. 799–858.
51. Arancibia-Zúñiga, A.; Carlesi, C.; Chamy, R.; Morales, J. Valorization of Copper Slag Through Alkali-Activated Materials: A Systematic Review. *Sustainability* **2026**, *18*, 4924. [CrossRef]
52. Mendoza, M.M.Q.; Cabanillas, F.S.; Vasquez, N.R.S.; Chumacero, J.M.G. Study on the Compaction and Strength Characteristics of High-Plasticity Clay Soil Using the Combined Application of Copper Slag and Recycled Glass Powder as Stabilizing Agents. *Int. J. Pavement Res. Technol.* **2026**. [CrossRef]
53. Sridhar, H.N.; Kumar, G.S.; Ramaraju, H.K.; Shreyashree, Y.; Pandit, P. Enhancing the Properties of Lateritic Soil Using Industrial Waste as an Alternative to Cement in Pavement Construction. *Discov. Mater.* **2026**, *6*, 5. [CrossRef]

Disclaimer/Publisher's Note: The statements, opinions and data contained in all publications are solely those of the individual author(s) and contributor(s) and not of MDPI and/or the editor(s). MDPI and/or the editor(s) disclaim responsibility for any injury to people or property resulting from any ideas, methods, instructions or products referred to in the content.